Original Article

Production of Corrosion Inhibitors Based on Crotonaldehyde and their Inhibitory Properties

Nurilloev Zafar[1], Beknazarov Khasan[2], Nomozov Abror[3]

[1]*Bukhara Institute of Engineering and Technology,*
[2,3]*Tashkent Scientific Research Institute of Chemical Technology, Shuro Bazaar, Tashkent district, Tashkent region, Republic of Uzbekistan*

[1]zafarnurilloyev@mail.ru

Abstract - *This paper studied the synthesis of oligomer-type corrosion inhibitors IKF-1 and IKF-2 based on crotonaldehyde, diamidophosphate and dithioamidophosphate. Therefore, the kinetics of the formation of this corrosion oligomer has been studied. The IR spectra of the obtained oligomer were studied and analyzed. The resulting oligomer was used as a corrosion inhibitor to protect metal structures from H_2S corrosion generated in the sulfur gases and petroleum industries. Integration efficiency was considered at different concentrations (100, 200, 300 and 500 mg / l) and temperatures (298 K and 323 K). The results were studied by SEM, EIS, gravimetric method, potentiostat polarization curves and enthalpy adsorption.*

Keywords - Diamidophosphate, Dithioamidophosphate, Croticaldehyde, Oligomer, IKF-1, IKF-2.

1. Introduction

The use of corrosion inhibitors represents an important option for the control of corrosion processes and for providing corrosion protection to different metals. Inhibitors have been widely used for corrosion control. They can be employed in a solution to control a corrosive media's aggressiveness. Moreover, they can be deposited on metal substrates or incorporated in different types of pre-treatments and coatings to retard or possibly avoid the onset of corrosion[1].

Today, oil and natural gas from fossil fuels meet about 60% of energy needs. The corrosion process is causing serious economic and moral damage to metal structures in the oil and gas industry. Its economic loss for the pipelines alone is estimated at $ 1,372 billion annually, of which $ 589 million is allocated to surface pipelines, $ 463 million to good pipelines, and $ 320 million to capital expenditures[2].

Corrosion in oil fields occurs at all stages, from wells to surface equipment. For example, in tanks, pipe casings, pipelines and other devices[3].

Cracking and processing for the production of petroleum and natural gas, high-quality fuels, oils, special fluids, additives and synthetics, platforming, isomerization, catalytic reforming and alkylation processes for the production of aromatic hydrocarbons and high-octane gasoline. The above processes use various corrosion inhibitors to protect against corrosion in the most sensible ways[3]. The inhibitory efficacy of copolymers based on maleic anhydride with 2-propenylphenol, modified by diethylamine and diethanolamine, was tested for water-salt systems for St.3 steel[4,5]. "N, N, N′, N″, N‴- pentamethyl diethylenamine-N, N ″ -di [tetradesilammonium bromide] 14-2-N (CH_3) -2-14 oligomers are used to protect steel(St20) from environmental corrosion[6–9]. The inhibitory efficiency of N- (3- (dimethyl-amino) propyl palmitate bromide compound for API N80 steel was studied at 25-60 ° C, and thermodynamic, electrochemical impedance spectroscopy and Langmuir adsorption were studied [10,11].

IKB-4 corrosion inhibitor is highly effective in inhibiting pipes in mineral-rich wells in oil fields [12][13]. Oligomer-type corrosion inhibitors and phosphate geopolymer-type compounds are highly effective corrosion inhibitors [13]. (3methacryloxypropyl) The inhibitory efficiency of a chemical compound based on hydrolytic condensation from modes such as trimethoxysilane and tetraethoxysilane and TEOS modification is high for electrochemical corrosion resistance and NO_2, SO_2 and H_2O environment[14].

Seabed steel technologies are the most vulnerable to corrosion. Therefore, it was found that the corrosion rate is 1 mm/y when the concentration of the quaternary amine salt of alkyl pyridine benzyl chloride is mainly used to increase the corrosion resistance of oil pipelines, which is 500 mg / L[15].

For saline waters saturated with carbon (IV) oxide to prevent corrosion of Q235 steel, the following 1- (2- thiourea) -2-alkyl imidazole (TAI) and chloride-1- (2,3-

hydroxypropyl) - 1- (2-thioureaethyl) -2-alkyl-imidazoline sodium phosphate has been used as a highly effective inhibitor of chemical compounds. The results were confirmed by electrochemical impedance spectroscopy (EIS) and surface analysis methods [16]. A chemical compound synthesized based on b-cyclodextrin grafted polyacrylamide (b-CD-PAM) for use in a sulfuric acid environment (X80 steel) in the oil and gas industry was tested in 1M H_2SO_4 solution as a green corrosion inhibitor. The inhibitory efficacy of the b-CD-PAM inhibitor was tested at different concentrations and temperatures. It was also examined by the gravimetric method, potentiodynamic polarization, scanning electron microscopy (SEM), and infrared methods. Based on the results obtained, it could be said that b-CD-PAM can be used as a highly effective inhibitor to prevent X80 steel corrosion in a sulfuric acid environment[18]. Ammonium salts of dithiophosphate o, and o-diesters, synthesized using white phosphorus, sulfur, alcohols, phenols, and amines, were used to protect light steel-based materials from CO_2 corrosion. It was found that the inhibitory efficiency of this corrosion inhibitor ranged from 90% to 99% for CO_2 and 88-89% for H_2S. "The effectiveness of most corrosion inhibitors known to us decreases with increasing temperature, but the corrosion's inhibitory effectiveness, as mentioned above, has also shown high efficiency in the temperature range of 30 ° C to 80 ° C[19,20].

Corrosion inhibitors synthesized based on amino acids L-cysteine, L-histidine and thiourea have been studied to be highly effective in inhibiting steel in carbon dioxide environments[21].

2. Materials and Methods

2.1. Materials

Crotonaldehyde, diamidophosphate and dithioamidophosphate were used to synthesise IKF-1 and IKF-2 brand corrosion inhibitors.

The inhibition efficiency of the corrosion inhibitor was studied in carbonate anhydride, hydrogen sulfide-saturated oil-field waters and hydrochloric acid environments.

The following brand (St. 20) steel with a size of 20x50x2 mm and a steel sample containing the following was used for the practical experiment: Fe 97,755-97,215%, C 0,17-0,24%, Si0,17- 0.37%, Mn0.35-0.65%, Ni up to 0.3%, S up to 0.04%, P up to 0.035%, Cr up to 0.25%, Cu up to 0.3%, As up to 0.08%.

2.2. Methods

Determination of the molecular mass of synthesized oligomers. The corrosion behaviour of steel (St.20) samples

in an acidic environment with inhibitors and without inhibitors was determined by the methods of polarization curves, polarization resistance, and the gravimetric method according to the mass loss of the sample after corrosion tests.

2.3. Preparation of oligomeric corrosion inhibitors based on crotonaldehyde with diamidophosphate (IKF-1) and dithioamidophosphate (IKF-2).

In synthesising nitrogen-, phosphorus, and sulfur-containing oligomeric corrosion inhibitors in ethanol, the reaction first proceeds with the formation of monomers based on crotonaldehyde with di(thio)amidophosphates. These monomers are oligomerized according to the following scheme:
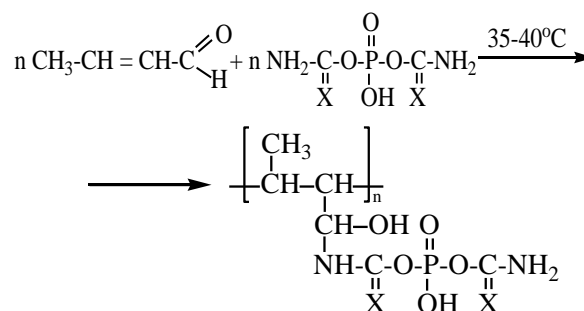
The ratio of crotonaldehyde and thiocarbamide is 1:2. The reaction is carried out in a thiocarbamide solution at a temperature of 308-313 K. Initially, 55-70% (thio)urea is introduced, after which the product is cooled. The remaining (thio)urea is added.

The resulting product of the interaction of crotonaldehyde with diamidophosphates has the following characteristics: a brown solid, non-volatile, the content of the main component is 98.7%, and impurities - 1.3%. The resulting product is diluted to 50-55% to obtain a working solution.

With an increase in the reaction temperature from 333 to 373 K at a constant ratio of reagents, it led to an increase in the yield of the oligomer; a further increase in temperature contributes to greater uniformity of the oligomer and also caused a slight increase in the molecular weight(viscosity) of polycrotonolamide phosphate from 0.06 to 0.12 dL/g. The identified features are probably associated with forming formaldehyde biradicals during heating.

To obtain polycrotonoamidophosphate of higher molecular weight, the reagents should be taken in equimolar ratios.

Table 2.1. Influence of the ratio of initial reagents on the composition of the resulting product (T=373 K, τ=2 hours).
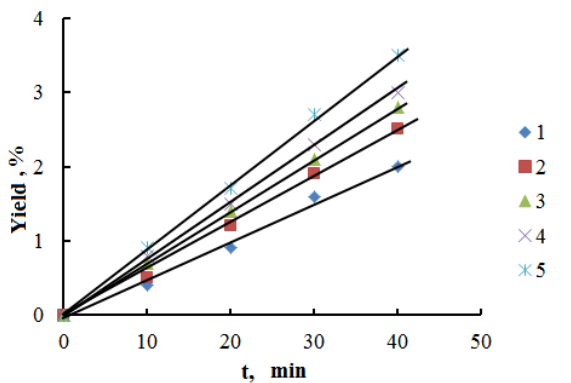
The ratio of crotonaldehyde + di (thio) amidophosphate	Output, %	Elemental analysis					
		Nitrogen		Phosphorus		Sulfur	
		Calculated	Found	Calculated	Found	Calculated	Found
1:3	53,6	9,79	9,61	10,08	10,01	22,3	21,98
1:2	74,3		9,59		10,03		21,76
1:1	89,4		9,74		10,07		22,29
2:1	79,6		9,69		10,05		22,13
3:1	65,4		9,62		10,04		21,87

The oligomer yield's dependence on the initial reagents' ratio is extreme, and the maximum yield corresponds to a ratio of 1:1 (Fig. 2.1.).

The study of the dependence of the reaction rate of the obtained substances, determined by the rate of consumption of di(thio)amidophosphate, on the ratio of the initial reagents, showed that the kinetic dependence of the formation of the oligomeric product is characterized by a decrease in the tangent of the slope angle in case of violation of equimolality (Fig. 2.2.).
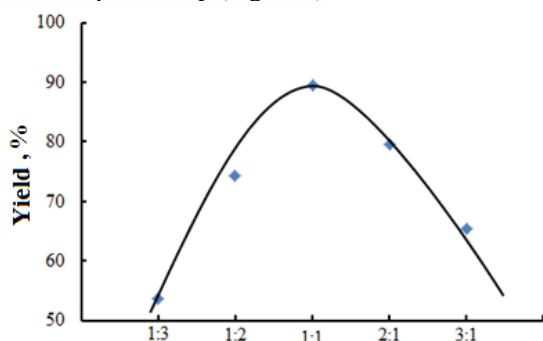
Crotonaldehyde. dithioamidophosphate
Fig. 2.1 Dependence of polymer yield on the ratio of initial substances. T=373 K, time 2 hours

1-1:3; 2-1:2; 3-3:1; 4-2:1; 5-1:1
Fig.2.2 Kinetic dependence of the reaction in the system
Crotonaldehyde. dithioamidophosphate in ethanol.
(T=373K).

2.4. Determination of the molecular mass of synthesized oligomers

In cryoscopic measurements, a Beckmann differential thermometer is used, which must first be set to the temperature range used. It should be noted that if the Beckmann thermometer is handled carelessly, a drop of mercury may fall into the upper tank of the thermometer and have to be adjusted again. For accurate measurements, it is necessary that the cooling of the investigated liquid occurs as slowly as possible. An air gap is used between the outer and inner test tubes. The test liquid must be constantly stirred during the experiment for its uniform cooling.

According to the obtained value of lowering the solution's crystallisation temperature, the solute's molecular weight is calculated by 2.1 formulas.

$$M = K \frac{1000 \cdot g_2}{g_1 \cdot \Delta t_{kp}} \qquad (2.1)$$

where: K – cryoscopic constant of water (K=1,86); g_1 – solvent mass; g_2 – the mass of the solute. Using the obtained and true values of the molecular weight, the relative error of its determination is calculated and compared with the maximum error according to the method.

Table 2.2. The value of the molecular weight of the synthesized oligomers

№	Oligomer	Molecular mass	Brutto formula (elementary link)
1	IKF-1	3620	$C_6N_2PO_7H_{11}$
2	IKF-2	3570	$C_6N_2S_2PO_5H_{11}$

2.5. Polarization curve method.

The polarization curves of a steel electrode in various media in the presence of various inhibitors at various temperatures and ratios were studied on a PI-50.1.1 potentiostat with a PR-8 programmer and a PDA-1 potentiometer.

During the experiments, the working electrode area was selected based on the capabilities of the potentiostat and the maximum currents in the region of active dissolution of steel. Before the experiment, the electrodes were actively cleaned with fine sandpaper, and then the surface was degreased with ethyl alcohol and washed many times with distilled water. The electrode leads were connected to the corresponding stamps of the potentiostat, and the device was put into working condition. The stationary potential of the working electrode was recorded using a cathode voltmeter. To record the dependence of the anode or cathode currents on the potential in the automatic potential sweep mode, an appropriate program was set using a PR-8 programmer. The PDA-1 two-coordinate potentiometer connected to the potentiostat was switched on. The required ranges of current (x-axis) and potential (y-axis) were selected in such a way as to fit the entire curve onto a recorder sheet. The initial position of the recorder's pen was set with zero-setting knobs. The value of the stationary potential was set on the programmer, and the potentiostat was brought into the switched-on cell mode. Under conditions when a potential corresponding to the stationary state is applied to the electrode, there should be no current through the cell. It can be checked with an ammeter connected to a potentiostat and by the absence of a deflection of the recorder's pen in the direction of the coordinate. After carrying out the specified preparatory work, the potential sweep was turned on, and the recorder began to record the i_c, E-curve. To determine the (specified) stationary rate of the metal dissolution (corrosive current)", the cathodic and anodic polarization curves were recorded near the stationary potential.

Based on the data of polarization measurements near the stationary potential, using linear extrapolation of the obtained curves, the corrosion current and the slope of the polarization curves of hydrogen evolution and metal dissolution were determined[21,22].

Thus, the rate of dissolution of the metal (corrosion current) i0c, which corresponds to the stationary potential Est, as well as the corrosion current ic, in the presence of inhibitors, which corresponds to the stationary potential Est, was determined. Also, comparing the values of the corrosion current found in various media and inhibited solutions, the effectiveness was evaluated for inhibitors - film formers and passivators. Using the following formulas (2.2, 2.3), the values of the braking coefficient γ were found, and the degree of protection Z % was calculated.

Deceleration coefficient $\quad \gamma = \dfrac{i_c}{i_c^0} \qquad$ (2.2)

degree of protection $Z = \dfrac{i_c - i_c^0}{i_c} 100\% \qquad$ (2.3)

where: i_c and i^0_c are the corrosion currents in the presence and absence of an inhibitor, respectively.

2.6. Gravimetric method

Experimental work was also carried out to determine the corrosion rate of a steel electrode in various media in the presence of the investigated inhibitors at their various concentrations and ratios in a certain temperature range by the gravimetric method. After holding the samples for 320 h, the corrosion products were removed with a scalpel and gravimetrically determined the corrosion rate (K) and corrosion losses (X) related to a blank experiment (corrosion in an inhibitor-free solution).

$$K = \frac{(m_1 - m_2) \cdot 1000}{S \cdot \tau_1} [\, mg/(m^2 day)] \qquad (2.4)$$

$$X = \frac{K_{инг}}{K_0} \cdot 100, \quad Z = 100 - X, \% \qquad (2.5)$$

where: m_1 is the mass of the metal plate before exposure, mg: m_2 is the mass of the metal plate after exposure, mg: S is the area of the metal plate, m^2: τ_1 is the exposure time, days.

3. Results and Discussion

3.1. IR spectral analysis of corrosion inhibitors IKF-1 and IKF-2

The structure of this compound was confirmed by UV, IR spectral and elemental analysis. IR spectra were recorded on a SHIMADZU instrument. The method of suspending substances in tablets with potassium bromide was used for samples. The IR spectrum of the obtained compound contains bands in the region of 3332 cm^{-1}, corresponding to the amide –CO–NH– groups. Free hydroxyl and bound CO– groups are characterized by the presence of bands in the IR spectra in the regions of 1446, 1373, 1334 and 1139, 1087, 1031, and 1001 cm^{-1}, respectively; the appearance of bands in the region of 1573 cm^{-1} indicates bound –CO–NH– groups. Free and bound P=O groups appear at 1244 and 2341 cm^{-1}.

3.1.1. The IR spectrum of the synthesized oligomer Which named after corrosion inhibitors IKF-2.

IR spectrum of polycrtonoldithioamidophosphate named after IKF-2. In the IR spectrum, bands of bound (thio)amides –CS–NH– appear in the region of 1517 cm^{-1}, which proves the reaction between crotonaldehyde and di(thio)amidophosphate. Free hydroxyl groups and bound CO– groups appear at 1452, 1396, 1344, 1305 and 1101, 1058 cm^{-1}. Amide NH$_2$– groups appear in the region of 3207 cm^{-1}. These groups mainly appear in the region of 1193 cm^{-1}.

3.2. Investigation of the protective properties of oligomeric inhibitors of hydrogen sulfide and carbon dioxide corrosion of steel

Corrosion tests were carried out in sealed vessels with a capacity of 500 ml on samples of steel St20 with a size of 30×15×2 mm for 24, 240 and 720 hours. The protective efficacy of the synthesized inhibitors (IKF-1 and IKF-2) was calculated by 3.1, the formula

$$Z = \frac{K_0 - K}{K_0} \cdot 100$$

$$(3.1)$$

where K_0 and K are the corrosion rates in non-inhibited and inhibited solutions, respectively.

In experiments with overpressure of CO_2, a sealed plastic cell was used. Polarization was carried out from the cathode to the anode region with a holding time of 30 s at each potential.

The pH value in the background solution without additives is 3.5. Integrating carbon dioxide (105 Pa) and 400 mg/l of hydrogen sulfide separately practically does not change the pH. In inhibited solutions, the pH is 5.0 and 5.8.

The surface of the samples was visually assessed; in non-inhibited background solutions, the steel samples darkened after 24 hours of testing with the appearance of structure-selective corrosion, which is more pronounced

after 10- and 30-day tests. In acidic media with H_2S additives and the presence of CO_2 and H_2S, the surface of the electrodes after daily tests is covered with a black deposit, which is easily removed with a rag. Still, during longer experiments, subsurface corrosion develops in addition. The introduction of synthesized inhibitors prevents the development of these types of corrosion.

The values of the corrosion rate in oil-field water and with the addition of CO_2 are close, and the introduction of H_2S (400 mg/L) + CO_2 (105 Pa) and H_2S (400 mg/L) noticeably increases the aggressiveness of the medium, which is consistent with previous studies research. It is due to the participation of both acid additives in the role of additional cathode depolarizers.

Table 3.1 Corrosion rate K, g/(m²day), protective efficiency Z, %, oligomeric inhibitor IKF-1 (200 mg/l) in oil-field water (OW) in the absence and presence of CO₂ and H₂S together and separately, St20 in inhibited solutions

τ, h	Indicators	Среда			
		Oil-field water (OW)	OW + H_2S (400 mg/l)	OW + CO_2 (10^5 Pa)	OW + H_2S (400 mg/l) + CO_2 (10^5 Pa)
24	K_0	0,314	0,519	0,307	0,536
	K	0,027	0,067	0,032	0,072
	Z	91,4	87,1	89,57	86,5
240	K_0	0,119	0,234	0,116	0,237
	K	0,008	0,018	0,005	0,035
	Z	93,2	92,3	95,6	85,2
720	K_0	0,0535	0,0965	0,0547	0,127
	K	0,0048	0,0089	0,0059	0,007
	Z	91,02	90,7	89,2	94,4

Table 3.1 shows that the protective effect of the corrosion inhibitor IKF-1 (200 mg/l) during daily tests in environments with H_2S and CO_2 and H_2S together is not high but slightly increases with increasing exposure time of the samples to τ = 720 hours. However, in inhibited solutions, the corrosion rate decreases with time, corresponding to 2 points on a ten-point scale of corrosion resistance, that is, the metal from the group of reduced resistance, which corresponds to 3 points after daily tests in

inhibited solutions containing H_2S and CO_2, passes into the group of resistant after 720 hours. IKF-2 (Table 3.2) exhibits higher values of the degree of protection Z in solutions with all acid additives, which is associated with forming stronger protective films on the steel surface. In the original oil-field water, Z does not exceed 92.5%, and it becomes even lower in the presence of CO2. Only in the presence of H_2S + CO_2 additives in the solution does the protective effect somewhat decrease, and to a greater extent, the longer the experiment.

Table 3.2. Corrosion rate K, g/(m²·h), protective efficiency Z, %, IKF-2 (200 mg/l) in oil-field water in the absence and presence of CO₂ and H₂S jointly and separately, St20 in inhibited solutions

τ, ч	Indicators	flow			
		Oil-field water (OW))	OW + H_2S (400 mg/l)	OW + CO_2 (10^5 Pa)	OW + H_2S (400 mg/l) + CO_2 (10^5 Pa)
24	K_0	0,564	0,126	0,117	0,465
	K	0,042	0,011	0,01	0,055
	Z	92,5	91,2	91,4	88,1
240	K_0	0,403	0,235	0,202	0,315
	K	0,036	0,022	0,02	0,034
	Z	91,0	90,6	90,0	89,2
720	K_0	0,435	0,565	0,321	0,542
	K	0,065	0,083	0,038	0,074
	Z	85,0	85,1	88,1	86,3

An analysis of the potentiostatic polarization curves showed that in oil-field water without additives, all the studied inhibitors slow down the cathodic process and facilitate the anode process near the corrosion potential, except for IKF -2, which slows down the anode process in the entire range of the studied potentials, shifting Ecor to the positive side, while, as other inhibitors shift it to the negative region (Fig. 3.1). In the presence of H₂S (Fig. 3.2),

all inhibitors slow down both partial electrode reactions. It causes an increase in their protective effects in hydrogen sulfide-containing media. In the presence of CO2 (Fig. 3.3), IKF-1 facilitates the cathodic reaction near the corrosion potential and significantly slows down the anodic one. Apparently, the facilitation of the anodic process during the deceleration of the cathodic process determines the low protective effect in solutions containing CO_2.
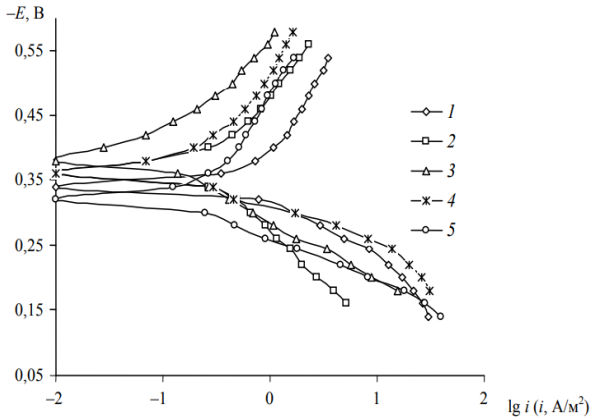

Fig. 3.1. Potentiostatic polarization curves for St20 in formation water: 1 – without additives; 2 – in the presence of 200 mg/l IKF -1; 3 - in the presence of IKF-2; 4 - in the presence of IKF-3; 5 - in the presence of IKF-4
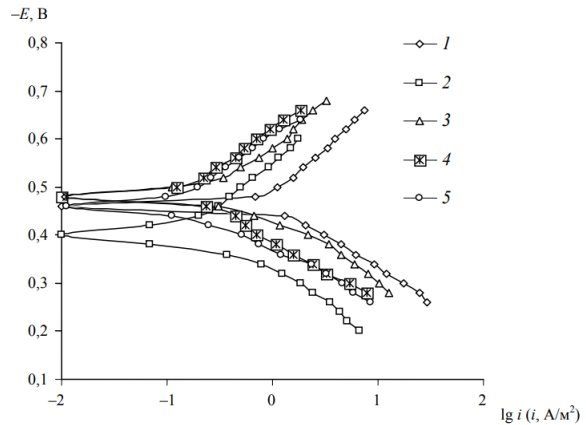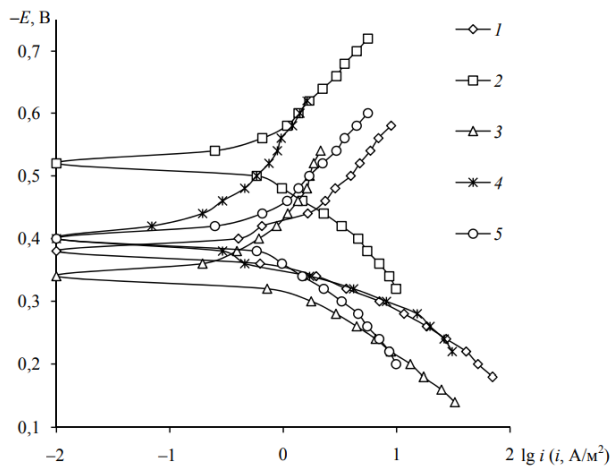

Pic. 3.2. Potentiostatic polarization curves for St20 in oil-field water saturated with H₂S (400 mg/l): 1 – without additives; 2 – in the presence of 200 mg/l IKF-1; 3 - in the presence of IKF-2; 4 - in the presence of IKF-3; 5 - in the presence of IKF-4

Fig. 3.3. Potentiostatic polarization curves for St20 in oil-field water saturated with CO2 (10⁵ Pa): 1 – without additives; 2 – in the presence of 200 mg/l IKF -1; 3 - in the presence of IKF-2; 4 - in the presence of IKF-3; 5 - in the presence of IKF-4.

inhibitors inhibit the diffusion of hydrogen into steel in oil-field water saturated with hydrogen sulfide and carbon dioxide separately and together and also contribute to preserving the plastic properties of St20 steel after exposure to solutions compared to uninhibited media.

3.3. Study of kinetic regularities and effective inhibition of steel corrosion in hydrochloric acid

The effect of IKF-1 and IKF-2 inhibitors in preventing corrosion of St20 steel in 0.5 M HCl was primarily tested using weight loss measurements at 303 K after 24 hours of immersion. The weight loss of St20 steel specimens before and after immersion can be used to evaluate corrosion parameters such as corrosion rate (CR) and inhibition efficiency (IE) at various concentrations using the following (3.2. and 3.3.)equations, and the results are shown in Table 3.3.

$$CR = \frac{\Delta W}{A \cdot t} \qquad (3.2)$$

$$IE = \frac{w_0 - w_i}{w_0} \times 100 \qquad (3.3)$$

where ΔW is the weight loss before and after immersion in an aggressive solution, W_0 and W_i - weight loss in the absence and presence of the inhibitor, respectively.

IKF-1 inhibitors IKF-2, compared with another type of corrosion inhibitor named after IKF-3 and IKF-4, when introduced into oil-field water at a concentration of 200 mg/l, reduce corrosion losses of carbon steel St20 within 30 days to 0.01…0.03 g/(m²· h). In hydrogen sulfide-containing media, IKF-1 and IKF-2 are the most effective. An increase in protective effectiveness accompanies an increase in the concentration of inhibitors to 1 g/l. In oil-field water without acid additives, the studied inhibitors slow the cathode process and facilitate the anode process. In the presence of H₂S, inhibition of both electrode reactions is observed, and when CO₂ solutions are saturated, only the cathodic one is observed. The studied

Table 3.3 confirmed the inhibitory ability of IKF-1 and IKF-2 as an anti-corrosion agent against steel in 0.5 M HCl. The corrosion rate decreases significantly after the introduction of IKF-1 and IKF-2 into an aggressive environment. The inhibition efficiency increases, and the

corrosion rate decreases with increasing inhibitor concentration. This characteristic behavior is graphically presented in (Figures 3.4 and 3.5) and can be explained by an increase in the adsorption of inhibitors with a

pronounced protection coating on the surface of St20 steel with an increased inhibitor concentration. This adsorption can be explained by the presence of various heteroatoms, multiple bonds, and functional groups in IKF-1 and IKF-2.

Table 3.3. Weight loss parameters during corrosion of steel St20 in 0.5 M HCl in the absence and presence of various concentrations of IKF-1 and IKF-2

Inhibitor	Inhibitor concentration, mg/l	Weight loss, mg	corrosion rate, mg/sm^{-2}·hour^{-1}	Inhibitory efficiency, %
Background	0	748,6	8,641	-
IKF-1	100	126,7	1,647	80,93
	200	78,3	0,9576	88,91
	300	50,4	0,5994	93,06
	500	38,7	0,4224	95,15
IKF-2	100	127,3	1,543	82,14
	200	79,8	0,9587	88,90
	300	52,6	0,5996	93,06
	500	39,4	0,4235	95,09

The results of calculations for the background and inhibited solutions of the values of the stationary potential (Est.), Corrosion current (i$_c$), braking coefficient (γ) and degree of protection (Z) at different temperatures are given in Table 3.4.

Experiments have shown that extremely dilute solutions of individual inhibitors show a high protective effect at a concentration of 300 mg/l. A comparison of the inhibition coefficient values and the degree of protection of the synthesized inhibitors and the Puro-tech 1011A inhibitor used in the industry shows a slightly higher (Table 3.4) efficiency of the IKF -1 and IKF -2 inhibitors. With an increase in temperature, the protection efficiency of IKF-1 and IKF-2 inhibitors somewhat increases, indicating the complexing properties of these compounds and an increase in adsorption processes.
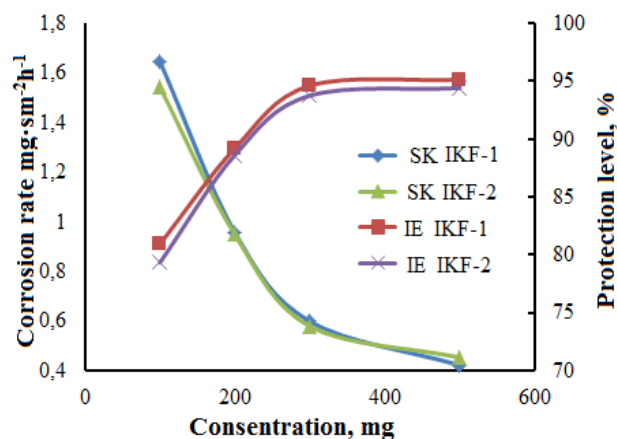
Fig. 3.4. Change in corrosion rate and degree of protection depending on the concentration of IKF-1 and IKF-2.

Table 3.4 Electrochemical parameters for the corrosion of steel St20 in 0.5 M HCl in the presence of IKF-1 and IKF-2 at various temperatures were obtained from potentiodynamic polarization studies.

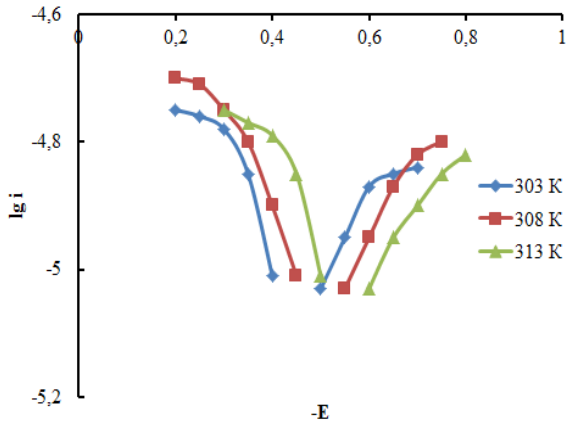| Inhibitor	T, ºC	C$_{inh.}$, mg/l	-E$_{st}$, B	i, мA/sm^2,	γ	Z, %
Background	25	–	0,870	375,20	–	–
IKF -1		300	0,535	22,02	17,03	94,13
IKF -2			0,530	22,35	16,78	94,04
Puro-tech 1011A			0,525	32,14	11,67	91,43
Фон	50	-	0,890	416,7	-	-
IKF -1		300	0,530	19,65	21,20	95,28
IKF -2			0,560	19,82	21,02	95,24
Puro-tech 1011A			0,553	20,86	19,97	94,99

Fig. 3.5. Polarization curves of a steel electrode at different temperatures in the presence of 100 mg/l of IKF-1 inhibitor in solution 0.5 M HCl.

When comparing the dependence of the inhibitory properties of the compounds on their structure, it turned out that the most effective corrosion inhibitors are IKF-1 and IKF-2 inhibitors. The inhibitor molecule contains branched alkyl groups and sulfur, nitrogen, and phosphorus heteroatoms, which enter into donor-acceptor interaction with metal surface atoms, forming chemical adsorption.

3.4. Adsorption isotherms

The contribution of inhibitor adsorption to corrosion inhibition is enormous. It was assumed that the inhibition of corrosion of steel St20 by IKF-1 and IKF-2 molecules occurs due to adsorption on the metal surface and is confirmed by weight loss and various electroanalytical estimates. Adsorption can be either physical adsorption via electrostatic interaction between ionic charges or dipoles on inhibitor molecules and interaction at the metal/solution interface or chemisorption involving charge transfer from inhibitor molecules to the metal surface to form a coordinate-type bond.

Various activation parameters such as apparent activation energy (E_a), apparent enthalpy of activation (ΔHa), and apparent entropy of activation (ΔSa), which provide further insight into the corrosion inhibition mechanism, have been explored in an Arrhenius-type plot and a transition state plot, which are mathematically expressed as follows equations

$$CR = Ae^{-E_a/RT} \qquad (3.4)$$

$$CR = \frac{RT}{Nh}e^{\frac{\Delta S_a^0}{R}}e^{\frac{-\Delta H_a^0}{RT}} \qquad (3.5)$$

where CR is the corrosion rate in mm/yr, A is the Arrhenius constant for the corrosion process, R is the universal gas constant, T is the Kelvin temperature, N is the Avogadro number, and h is the bar constant.

The Arrhenius plot of lnCR vs 1/T (Figure 3.6) and the transition state plot LnCR/T vs 1/T (Figure 3.7.) with regression coefficients of approximate unity can be used to estimate corrosion kinetic parameters. Table 3.5. shows various activation parameters such as Ea, ΔHa, and ΔSa obtained from the slope and intersection point of the Arrhenius plot and the transition plot for uninhibited and inhibited solutions containing various concentrations of IKF-1 and IKF-2. It was found that the values of E_a and the preliminary exponential Arrhenius coefficients are higher in the presence of an inhibitor, which indicates a slowdown in corrosion in the presence of IKF-1 and IKF-2 inhibitors. An increase in Ea values suggests that the inhibitor's molecular adsorption increases the energy barrier for corrosion molecules, which leads to a decrease in the corrosion rate. Higher E_a values in the inhibited system support the physical adsorption mechanism. In comparison, unchanged or lower E_a values for the inhibited systems than the background solution indicate the chemisorption mechanism. In the present study, the E_a values for inhibited solutions are higher than for non-inhibited solutions, suggesting a sorption mechanism for corrosion inhibition.

Table 3.5. Values of activation parameters for steel St20 in 0.5 M HCl in the absence and presence of IKF-1

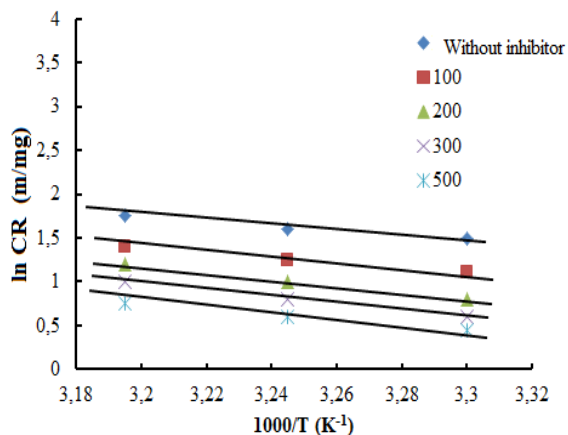| Concentration, mg/l	E_a, kJ/mol	ΔH_a, kJ/mol	ΔS_a^0, J/mol ·K	$E_a - \Delta H_a$
without inhibitor	42,46	38,90	38,35	2,55
100	57,89	56,23	18,64	2,56
200	103,78	101,36	43,41	2,56
300	98,65	92,64	36,54	2,56
500	103,34	100,68	41,37	2,56

Fig. 3.6. Arrhenius dependence for steel St20 in 0.5 M HCl in the presence and absence of the IKF -1 inhibitor.
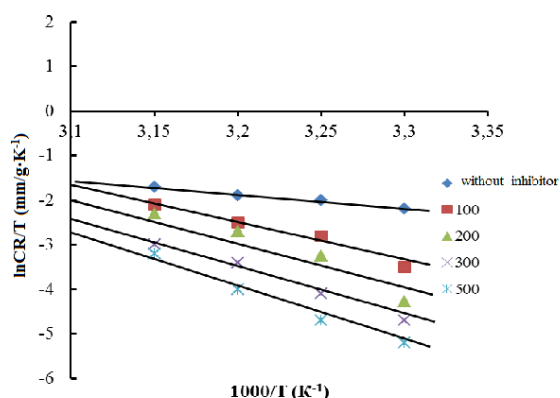

Fig. 3.7. Graph the transition state of steel St20 in 0.5 M HCl in the presence and absence of IKF-1.

A quick look at the ΔH_a values in Table 3.5 also shows that positive enthalpy values increase with concentration, indicating that the metal dissolution process is endothermic and requires more energy to reach an activated state or equilibrium. The average difference between E_a and ΔH_a for each inhibitor is about 2.56 kJ/mol, which is approximately equal to RT (2.63 kJ/mol), suggesting a unimolecular metal dissolution reaction. The entropy value ΔS_a is negative in the absence of an inhibitor but tends to become positive at higher concentrations of IKF-1. It can be interpreted in connection with the process of increasing disorder when the inhibitor molecule passes to the activated complex.

3.5. Calculation of parameters of adsorption isotherm and thermodynamics

The interaction mechanism between an inhibitor and a metal surface can be explained using adsorption isotherms. The degree of surface coverage, θ, was calculated for different concentrations of inhibitors from weight loss measurements as follows: g% = $\theta \cdot 100$, assuming a direct relationship between surface coverage and inhibition efficiency. The resulting surface coverage values were applied to various adsorption isotherm models, and the correlation coefficient (R_2) was a useful means of determining the best-fit isotherm. By far, the best result was obtained for the Freundlich adsorption isotherm, which can be formulated as:

$$\theta = K_{ads}C^n \quad (3.6)$$

or

$$log\theta = logK_{ads} + nlogC \quad (3.7)$$

where $0<n<1$; θ is the surface coverage, C is the inhibitor concentration, and K_{ads} is the equilibrium constant of the adsorption-desorption process. On fig. Figure 3.8 shows $log\theta$ versus $logC$ for (a) IKF-1 and (b) IKF-2, (at 30-60°C). Linear plots are obtained for the various systems studied, indicating that the Freundlich adsorption isotherm can approximate the experimental results regarding the adsorption of inhibitors. The adsorption parameters derived from the graph are shown in Table 3.6. The results in the table show that the values of Kads, which indicate the strength of the binding of the inhibitor to the metal surface, decrease with increasing temperature. This behavior can be interpreted as an increase in temperature leading to the desorption of some adsorbed functional groups of inhibitors on the metal surface and is consistent with the proposed physical sorption mechanism.

Adsorption free energy values indicate that the inhibitors function by physical adsorption on the metal surface. Typically, adsorption free energy values up to 20 kJ/mol correspond to an electrostatic interaction between charged molecules and a charged metal (indicating physical adsorption). In comparison, values more negative than 40 kJ/mol involve charge separation or transfer from molecules inhibitor to the metal surface to form a coordination type bond (indicating chemisorption). The results presented in the table show that the values of adsorption free energy for all studied systems lie between –9.8 and –10.7 kJ/mol, indicating spontaneous additives adsorption by the mechanism of physical sorption.

The thermodynamic model is very useful for explaining the phenomenon of the adsorption of an inhibitor molecule. The enthalpy of adsorption can be calculated according to the Wan't Hoff equation:

$$lnK_{ads} = \frac{-\Delta H^o_{ads}}{RT} + constant \quad (3.8)$$

where ΔH°_{ads} and K_{ads} are adsorption enthalpy and adsorption equilibrium constant, respectively.

On fig. 3.8 is a graph of the relationship between lnKads and 1/T for inhibitors of IKF-1 and IKF-2. Straight line graphs were obtained, and the enthalpy of adsorption was obtained from the slope of the line graph.

Table 3.6. Freundlich adsorption parameters for IKF-1 and IKF-2, inhibitors at different temperatures.

Inhibitor	Temperature, °C	$\Delta G°_{ads}$, kJ/mol^{-1}	n	R^2
IKF -1	30	-10,7	0,62	0,98
	40	-10,3	0,67	0,98
	50	-9,8	0,69	0,97
	60	-10,6	0,86	0,98
IKF -2	30	-10,2	1,02	0,97
	40	-10,2	1,04	0,98
	50	-10,4	1,03	0,99
	60	-10,5	1,05	0,99
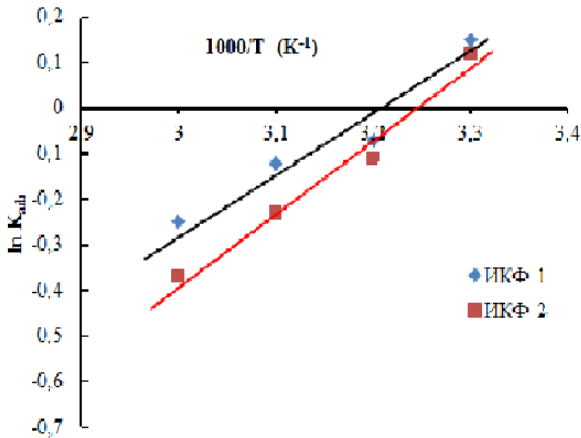
Fig. 3.8. Dependence of lnK$_{ads}$ on 1/T for inhibitors IKF-1 and IKF-2

The enthalpy of adsorption (ΔH) can be roughly considered the standard enthalpy of adsorption ΔH°ads under experimental conditions, and the obtained values were 22.5 and 16.1 kJ/mol for inhibitors IKF-1 and IKF-2 respectively. The standard adsorption free energy ΔG°ads given in Table 3.6 was obtained using the relationship:

$$\log K_{ads} = -\log C_{H_2O} - \frac{\Delta G^o_{ads}}{2.303RT} \quad (3.9)$$

where CH_2O is the water concentration expressed in g·l-1 (same as the inhibitor concentration), R is the molar gas constant, and T is the absolute temperature. The standard adsorption entropy (ΔS°ads) was derived from the basic equation of thermodynamics:

$$\Delta G^o_{ads} = \Delta H^o_{ads} - T\Delta S^o_{ads} \quad (3.10)$$

The calculated values of ΔS°ads were 0.039, 0.039, 0.037 and 0.035 J·mol-1·K-1 at 30, 40, 50 and 60°C, respectively, for IKF -1. The values–6.6×10^{-4}, –3.2×10^{-3}, –4.3×10^{-3} and –4.8×10^{-3} J·mol^{-1}·K^{-1} were obtained for IKF-2, respectively. The values of thermodynamic parameters for the adsorption of inhibitors can provide valuable information about the corrosion inhibition mechanism. The endothermic adsorption process (ΔH°ads> 0) is uniquely explained by chemisorption, while in general, the exothermic adsorption process (ΔH°ads<0) can involve either physical sorption or chemisorption or a mixture of both processes. In the present case, the negative sign of ΔH°ads indicates that the adsorption of inhibitors is an exothermic process. Negative values of ΔS°ads indicate that a decrease in entropy accompanies the adsorption process.

The negative values of ΔS°ads can be explained as follows: before adsorption, the functionally active groups of inhibitors on the surface of steel 20 could move freely in the bulk of the solution (the functionally active groups were chaotic), but over time, in adsorption, the functionally active groups of inhibitors were ordered. Adsorbed on the surface of steel St20, which led to a decrease in entropy.

The standard enthalpy of adsorption (ΔH°ads) can also be derived from the Gibbs-Helmholtz equation, expressed as:

$$\frac{\Delta G^o_{ads}}{T} = \frac{\Delta H^o_{ads}}{T} + \text{constant} \quad (3.11)$$
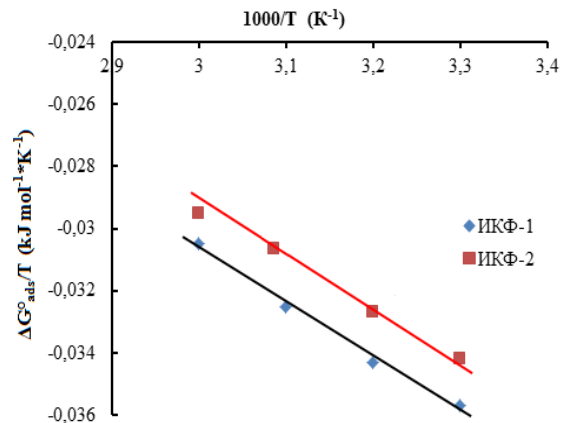
Fig. 3.9. Dependence of ΔG°$_{ads}$/T on 1/T for IKF-1 and IKF-2

Fig 3.9 shows the change in ΔG°ads/T from 1/T, which gives a straight line with a slope equal to ΔH°ads. It can be seen from the figure that ΔG°ads/T decreases linearly with 1/T.

The calculated ΔH°ads values using the Gibbs-Helmholtz equation are 22.6 and 16.9 kJ/mol-1 for IKF-1 and IKF-2 inhibitors, respectively, confirming the exothermic behavior of adsorption on the steel surface; therefore, the ΔH°ads values, obtained by both methods satisfy the Gibbs-Helmholtz equations.
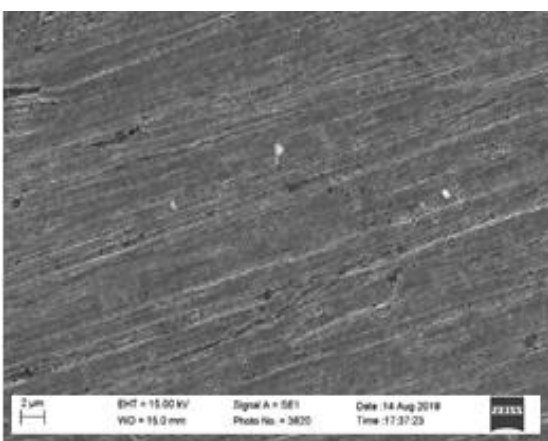
3.6. Scanning electron microscope (SEM)

It is assumed that the inhibition of corrosion in solution occurs due to the adsorption of the inhibitor on the metal surface. The nature of adsorption is determined by various factors, such as the type of aggressive medium, the nature and charge of the metal, the charge and dipole moment of the inhibitor, etc.
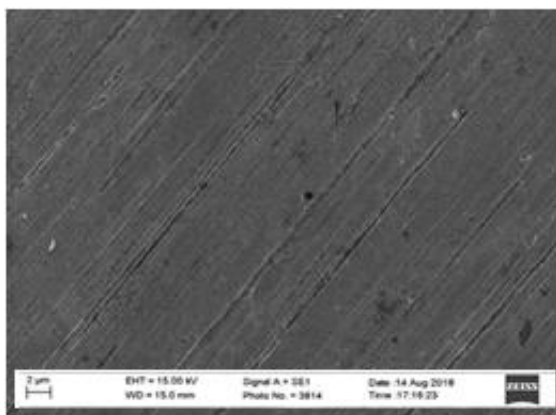
Pic.3.1. SEM micrograph of initial steel St20.
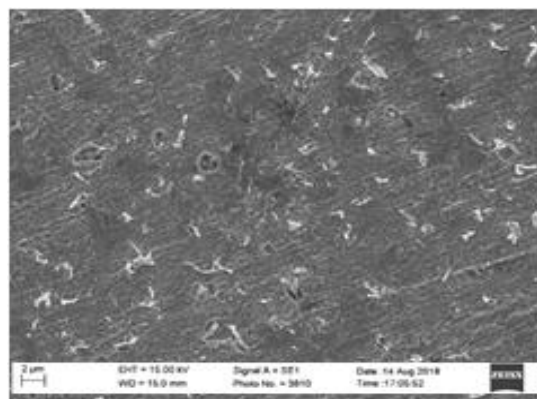
Pic.3.2. SEM micrograph of steel St20 in 0.5 M HCl.

Pic.3.1, 3.2 and 3.3 show scanning electron micrographs of the surface of abraded St20 steel immersed in 0.5 M HCl in the absence and presence of IKF-1 to confirm the effectiveness of IKF-1 as a corrosion inhibitor.

Pic.3.3. SEM micrograph of steel St20 in 0.5 M HCl + IKF-1.

SEM images were taken to assess the protective ability of IKF-1 against corrosion of St20 steel in 0.5 M HCl.

4. Conclusion

To determine the inhibition efficiency and mechanism of both (IKF-1 and IKF-2) corrosion inhibitors, corrosion rate, protection level, inhibition coefficient, and electrochemical and polarization curve methods were used.

The developed inhibitors IKF-1 and IKF-2 (corrosion inhibitors for circulating waters of increased corrosivity) are recommended for use in circulating and oil-field water of petrochemical enterprises to protect equipment made of carbon steel.

REFERENCES

[1] Andreatta F., Fedrizzi L. Corrosion Inhibitors / *Springer Ser. Mater. Sci*. Springer Verlag, vol. 233, pp. 59-84, 2016.

[2] Z. Panossian, N.L.d. Almeida, R.M.F.d. Sousa, G.d.S. Pimenta L.B.S.M, "Corrosion of Carbon Steel Pipes and Tanks by Concentrated Sulfuric Acid: A Review," *Corros. Sci,* no. 58, pp. 1-11, 2012. Doi:10.1016/j.corsci.2012.01.025

[3] M.M. Osman M.N.S, "Ome Ethoxylated Fatty Acids as Corrosion Inhibitors for Low Carbon Steel in Oil-Field Water," *Mater. Chem. Phys,* no. 77, pp. 261-269, 2003. Doi:10.1016/S0254-0584(01)00580-6

[4] Magerramov A.M. et al., "Synthesis of Co-Oligomers of 2-Propenylphenol with Maleic Anhydride and Study of Products of their Transformations with Amines as Steel Corrosion Inhibitors, *Russ. J. Appl. Chem,* Springer, vol. 87, no. 4, pp. 456-460, 2014.

[5] Beknazarov, K. S., Dzhlilov, A. T., Ostanov, U. Y., & Erkaev A.M, "The Inhibition of the Corrosion of Carbon Steel by Oligomeric Corrosion Inhibitors in Different Media," *Int. Polym. Sci. Technol*, vol. 42, no. 4, pp. 33-37. Doi:10.1177/0307174x1504200406.

[6] Alehyen S. et al., "Preparation of a New Oligomeric Surfactant: N,N,N′,N″,N″-Pentamethyl Diethyleneamine—N,N″-Di-[Tetradecylammonium Bromide] and the Study of its Thermodynamic Properties," *J. Surfactants Deterg*, Springer, vol. 13, no. 3, pp. 339-348, 2009.

[7] Bharatiya U. et al., "Effect of Corrosion on Crude Oil and Natural Gas Pipeline with Emphasis on Prevention by Ecofriendly Corrosion Inhibitors: A Comprehensive Review," *J. Bio- Tribo-Corrosion*, Springer, vol. 5, no. 2, pp. 112, 2019. Doi::10.1007/s40735-019-0225-9

[8] Chernov V.Y, "Influence of Oxygen and Hydrogen Sulfide on the Carbonic-Acid Corrosion of Welded Metal Structures of Oil and Gas Equipment," *Mater. Sci.,* Springer, vol. 37, no. 5, pp. 808-815, 2001.

[9] Ostanov, U. Y., Beknazarov, K. S., & Dzhalilov A.T, "Study by Differential Thermal Analysis and Thermogravimetric Analysis of the Heat Stability of Polyethylene Stabilized with Gossypol Derivatives," *J. Int. Polym. Sci. Technol*., vol. 38, no. 9, pp. 25-27, 2015. Doi:10.1177/0307174X1504200406

[10] Fouda A.S. et al., "Corrosion Inhibition of Novel Prepared Cationic Surfactants for API N80 Carbon Steel Pipelines in Oil Industries," *Surf. Eng. Appl. Electrochem,* Springer, vol. 54, no. 2, pp. 180-193, 2018.

[11] Beknazarov K.S. Dzhalilov A.T, "The Synthesis of Oligomeric Derivatives of Gossypol and the Study of Their Antioxidative Properties," *Int. Polym. Sci. Technol*., vol. 43, no. 3, pp. T25-T30, 2016.

[12] Gonik A.A., "Effect of a Diphilic Corrosion Inhibitor on the Iron Passivity in Oil-Field Electrolytes," *Prot. Met.* Springer, vol. 41, no. 2, pp. 173-176, 2005.

[13] Matienzo L.J. et al., "Environmental and Adhesive Durability of Aluminium-Polymer Systems Protected with Organic Corrosion Inhibitors," *J. Mater. Sci.,* Springer, vol. 21, no. 5, pp. 1601–1608, 1986.

[14] Wang D. et al., Enhancement Corrosion Resistance of (3methacryloxypropyl) Silsesquioxane Hybrid Films and its Validation by Gas-Molecule Diffusion Coefficients using MD Simulation," *J. Sol-Gel Sci. Technol,* Springer, vol. 49, no. 3, pp. 293-300, 2008.

[15] Rihan R., Shawabkeh R., Al-Bakr N. "The Effect of Two Amine-Based Corrosion Inhibitors in Improving the Corrosion Resistance of Carbon Steel in Sea Water," *J. Mater. Eng. Perform,* Springer, vol. 23, no. 3, pp. 693–699, 2014.

[16] Ugryumov O. V. et al., "Corrosion Inhibitors of the Snpkh Brand, 2, The P,N-Containing Corrosion Inhibitor for Protection of Oil-Field Equipment," *Prot. Met.* Springer, vol. 43, no. 1, pp. 87-94, 2007.

[17] Zhang J. et al., "Theoretical and Experimental Studies for Corrosion Inhibition Performance of Q235 Steel by Imidazoline Inhibitors against CO2 Corrosion," *J. Surfactants Deterg,* Springer, vol. 16, no. 6, pp. 947-956, 2013.

[18] Askari M. et al., "Downhole Corrosion Inhibitors for Oil and Gas Production – A Review," *Appl. Surf. Sci. Adv. Elsevier,* vol. 6, pp. 100128, 2021. https://doi.org/10.1016/j.apsadv.2021.100128

[19] Batyeva E.S. et al., "New, Effective Carbon Dioxide and Hydrogen Sulfide Corrosion Inhibitors Based on White Phosphorus, Sulfur, Alcohols, and Amines," *Pet. Chem.*, Springer, vol. 53, no. 2, pp. 139–143, 2013.

[20] Narzullaev, A.X, Beknazarov, X.S, Jalilov, A.T, Rajabova, M.F., "Studying the Efficiency of Corrosion Inhibitor IKTSF-1, IR-DEA, IR-DAR-20 in 1m HCl," *International Journal of Advanced Science and Technology*, vol. 28, no. 15, pp. 113-122, 2019.

[21] Zhang Q.H. et al., "Comparison of the Synergistic Inhibition Mechanism of Two Eco-Friendly Amino Acids Combined Corrosion Inhibitors for Carbon Steel Pipelines in Oil and Gas Production," *Appl. Surf. Sci. North-Holland,* vol. 583, pp. 152559, 2022. doi: 10.1016/j.apsusc.2022.152559

[22] J.A.A. Yamin, E.Ali Eh Sheet and A. Al-Amiery, "Statistical Analysis and Optimization of the Corrosion Inhibition Efficiency of a Locally Made Corrosion Inhibitor Under Different Operating Variables Using RSM," *Int. J. Corros. Scale Inhib*., vol. 9, no. 2, pp. 502-518, 2020. doi: 10.17675/2305-6894-2020-9-2-6

[23] Firoz Ahmed, Md. Saifur Rahman, Md. Ibrahim H Mondal, "Cotton Fibre Functionalization With Prepared Carboxymethyl Chitosan From Prawn Shell Waste: An Eco-Friendly Approach," *International Journal of Polymer and Textile Engineering*, vol. 8, no. 1, pp. 9-14, 2021. *Crossref,* https://doi.org/10.14445/23942592/IJPTE-V8I1P103